



## Research article

# Comparative proteome analysis of *Brettanomyces bruxellensis* under hydroxycinnamic acid growth



Lourdes Carmona<sup>a,b,1</sup>, Javier Varela<sup>a,1</sup>, Liliana Godoy<sup>a,1</sup>, María Angélica Ganga<sup>a,b,\*</sup>

<sup>a</sup> Laboratory of Biotechnology and Applied Microbiology, Department of Food Science and Technology, University of Santiago of Chile, Obispo Umaña 050, Estación Central, Santiago, Chile

<sup>b</sup> Millennium Nucleus for Fungal Integrative and Synthetic Biology (MN-FISB), 120043, Chile

## ARTICLE INFO

## Article history:

Received 15 March 2016

Accepted 26 June 2016

Available online 13 August 2016

## Keywords:

Ethylphenols

Metabolic flux regulation

Proteomics

Spoilage yeast

Wine alterations

Wine industry

## ABSTRACT

**Background:** *Brettanomyces bruxellensis* is an important spoilage yeast in the winemaking process. The capacity of this yeast to generate an undesired off-flavor constitutes a significant loss in the Chilean wine industry.

**Results:** The proteomic profile of *B. bruxellensis* in the presence of *p*-coumaric acid was determined by 2D gel electrophoresis, gel image analysis and differential spot selection. A set of 41 proteins showed a differential accumulation of  $\pm 2$  and a *p*-value  $\leq 0.0001$ . The homology sequence analysis was performed using the databases available. Differential proteins belonged to the categories of 'energy production and conversion' and 'amino acid transport and metabolism'.

**Conclusions:** The proteomic profile of *B. bruxellensis* cultivated in the presence of *p*-coumaric acid in synthetic wine, agrees with the hypothesis of metabolic flux regulation, allowing a better conditioning to an adverse environment. This study involved the translational level of *B. bruxellensis* in the production of ethylphenols and corroborated that this yeast presented an advantage in these stress conditions. Thus, this work will allow an understanding of the regulation and processes involved in the production of ethyl-derivate compounds by *B. bruxellensis*. Furthermore, it allows the development of newer and better techniques for spoilage yeast control.

© 2016 Pontificia Universidad Católica de Valparaíso. Production and hosting by Elsevier B.V. All rights reserved. This is an open access article under the CC BY-NC-ND license (<http://creativecommons.org/licenses/by-nc-nd/4.0/>).

## 1. Introduction

Wine alterations by yeast still constitute a potential threat, particularly for products aged in wood barrels, where there is an increased interest in spoilage by yeasts belonging to the genus *Brettanomyces*. Among the species of this genus, *Brettanomyces bruxellensis* is considered to be the worst contaminant not only in the wine industry, but also in other processes such as bioethanol production [1,2,3]. The presence of this yeast in wine has been associated with the appearance of phenolic aromas described as 'medical', 'horsy' or 'smoky', which are considered strongly detractive for the sensorial characteristics of the product. These off-odors result from the metabolization of hydroxycinnamic acids naturally present in grape must by *B. bruxellensis*. These hydroxycinnamic acids present antimicrobial effects since microorganisms metabolize them to much less toxic compounds such as vinyl or ethyl derivatives [4]. The latter are phenolic compounds such as 4-vinylphenol and 4-ethylphenol from *p*-coumaric acid, or 4-vinylguaiacol and 4-ethylguaiacol from

ferulic acid [3]. The mechanism of action of hydroxycinnamic acids is similar to that of weak acids, which can disturb intracellular pH and hence cell metabolism [5]. In order to counter the pH effects, the cells reduce the concentration of protons by using a proton pump (Pma1p) in the presence of different weak acids such as cinnamic, ascorbic, octanoic, succinic or acetic acids [6,7]. An increase of H<sup>+</sup>-ATPase pump activity has been described during the lag growth phase of *B. bruxellensis* in the presence of *p*-coumaric acid, suggesting an early adaptation mechanism against this hydroxycinnamic acid [8].

Different studies revealed that *B. bruxellensis* strains varied in their production of phenolic substances in wine [9,10]. This variability in sensory descriptions of *B. bruxellensis* has been related to genetic strain variation. In fact, it is known that this yeast is a highly diverse microorganism both genetically [11,12] and physiologically [9,13]. Genetic studies in this yeast have shown an unusual variability in chromosome number and genome rearrangements which confer the ability to survive and proliferate after alcoholic fermentation [11,14,15]. Studies of different *B. bruxellensis* strains (CBS) belonging to the same group display a very similar off-flavor production [9]. However, the isolates from Tuscan wines showed a wide biodiversity within the species, despite the limited geographic area [16]. This shows that the relationship between the genomic diversity of *B. bruxellensis* and its ability to produce phenols is still unclear.

\* Corresponding author.

E-mail address: [angelica.ganga@usach.cl](mailto:angelica.ganga@usach.cl) (M.A. Ganga).

<sup>1</sup> These authors contributed equally to this work.

Peer review under responsibility of Pontificia Universidad Católica de Valparaíso.

The *B. bruxellensis* strain LAMAP2480, an isolate from Chilean wines, displays a high production of phenolic compounds, representing a potential risk as wine-spoilage yeast. This isolate shows a very efficient adaptation mechanism against the action of *p*-coumaric acid during growth in synthetic wine [17].

Recently, genomic and transcriptomic approaches provided a set of genes in *B. bruxellensis* LAMAP2480 which is highly represented when the strain is grown in the presence of *p*-coumaric acid [18]. Thus, in order to elucidate the mechanism used by *B. bruxellensis* LAMAP2480 in 4-ethylphenol production, the objective of this work was to evaluate the proteomic response during yeast growth in the presence or absence of *p*-coumaric acid.

## 2. Materials and methods

### 2.1. Microorganism

*B. bruxellensis* LAMAP2480 was obtained from the strain collection of the Applied Microbiology and Biotechnology Laboratory (LAMAP) of the Universidad de Santiago de Chile (USACH). The strain was maintained on YPD medium (0.5% peptone, 0.5% yeast extract, 4% glucose, 4% agar, pH 6.0) until use.

### 2.2. Pre-culture and culture conditions

#### 2.2.1. Pre-culture conditions

Before performing synthetic wine assays, an adaptation step was carried out as described by Sturm et al. [19]. *B. bruxellensis* LAMAP2480 was grown in YPD medium for 10 d at 28°C. Colonies from YPD agar were inoculated into 10 mL of YPD1 (0.5% peptone, 0.5% yeast extract, 8% glucose, pH 6) supplemented with 6% (v/v) of ethanol and grown at 28°C for 48 h. A total volume of the inoculum was added to fresh medium prepared in a 1:1 proportion of SW (0.2% yeast extract, 0.12% glucose, 0.24% fructose, 0.06% trehalose, 0.1% (NH<sub>4</sub>)<sub>2</sub>SO<sub>4</sub>, 0.8% MgSO<sub>4</sub>, 0.2% KH<sub>2</sub>PO<sub>3</sub>, 0.25 mg/L of biotin, 0.0045 mg/l of thiamin, 10% ethanol (v/v), pH 3.8 adjusted with HCl), YPD2 (0.5% peptone, 0.5% yeast extract, 4% glucose, pH 4). The culture was incubated for 3 d at 28°C. Finally, 9 vol of synthetic wine was added to 1 vol of culture and yeasts were grown until a concentration of 10<sup>8</sup> cells/mL.

#### 2.2.2. Culture conditions

A volume from the adapted culture was used to inoculate synthetic wine to a final concentration of 10<sup>6</sup> cells/mL, containing 100 mg/L of *p*-coumaric acid (Sigma-Aldrich, USA). A control without acid was also used.

### 2.3. Growth kinetic

Growth of *B. bruxellensis* LAMAP2480 in synthetic wine in the presence or absence of *p*-coumaric acid was performed at 28°C for 8 d with shaking at 150 rpm. Growth was determined by measuring absorbance at 640 nm. A total of 6 biological replicates of each treatment were collected by centrifugation at exponential phase. The cell pellets were washed with ice-cool Milli-Q water, and stored at –80°C until protein extraction.

### 2.4. Protein extraction and quantification

Each sample of *B. bruxellensis* was submitted to protein extraction by a modified protocol [20]. Cultures of 100 mL were collected at exponential phase, six samples for each treatment: in the presence or absence of 100 mg/L of *p*-coumaric acid. Samples were thawed on ice and collected by centrifugation at 800 × g for 5 min at 0°C. The sediment was washed with 30 mL phosphate buffer saline (PBS: 140 mM NaCl, 2 mM KCl, 10 mM Na<sub>2</sub>HPO<sub>4</sub>, 1 mM KH<sub>2</sub>PO<sub>4</sub>, pH 4.0)

and incubated on ice for 10 min. Cells were then recovered by centrifugation at 800 × g for 5 min at 0°C. These wash and centrifugation steps were performed twice. Subsequently, cells were resuspended in 20 mL stabilization buffer A (1 M sorbitol, 10 mM MgCl<sub>2</sub>, 25 mM potassium phosphate buffer solution, pH 7.8; 10.2 g/mL phenyl-methyl-sulfonyl fluoride (PMSF), 2 mM dithiothreitol) and incubated at 30°C for 10 min. Following centrifugation at 800 × g for 5 min, the pellet was resuspended in 20 mL stabilization buffer B (1 M sorbitol, 10 mM MgCl<sub>2</sub>, 25 mM potassium phosphate buffer solution, pH 5.5; 10.2 mg/mL PMSF, 2 mM dithiothreitol) and incubated for 10 min at 30°C. Then, 20 µg/µL zymolyase (Seikagaku Corporation, Tokyo, Japan) was added and incubated at 37°C for 3 h. Once the spheroplasts were obtained, they were collected by centrifugation at 200 × g for 10 min at 4°C. The pellet was resuspended in 3 mL of lysis buffer (50 mM HEPES buffer solution, 17 mg/mL PMSF, 20 µg/mL aprotinin, 30 µL NP-40) and incubated on ice for 1 h. Finally, it was centrifuged at 6200 × g for 10 min at 4°C and the supernatant collected. The total protein concentration was determined using the method described by Bradford [21], using BSA as standard. To remove salts and other substances which could interfere with the labeling, electrophoresis and improve spot resolution, we used the Ettan 2-D Clean-up kit (GE Healthcare, 80-6484-51) to precipitate the proteins. Therefore, proteins were suspended in the DIGE labeling buffer (7 M urea, 2 M thiourea, 4% CHAPS and 20 mM Tris). Finally, the protein concentration was determined with the RC-DC (BioRad Protein Assay) method using BSA as standard. Integrity of proteins was checked in 12% SDS-PAGE gels.

### 2.5. Labeling protein and 2D gel electrophoresis

In order to prevent protein binding affinity to fluorochromes, the samples collected were labeled with fluorescent dyes using the minimal labeling technique. Half of the biological control samples and half of the treated samples were labeled with Cy3 and the other half were labeled with Cy5, by incubating 50 µg of proteins with 400 pmol of Cy3 or Cy5, respectively. The labeling reaction was conducted at 4°C in the dark for 60 min. An internal standard (IS), composed of equal amounts of all the samples, was labeled with Cy2.

Isoelectric focusing (IEF) was performed in 24 cm Immobiline Dry-Strips (BioRad), immobilized in a pH gradient 3–10 and hydrated in a rehydration solution (8 M urea, 4% CHAPS, DeStreak (12 µg/L), 65 mM DTT and 1% ampholytes (pH 3–11)). The IEF was performed at 20°C in the strips: i) 300 V for 4 h, ii) 1000 V for 6 h, iii) 8000 V for 3 h and iv) 8000 V–32,000 V/h. Strips were equilibrated through a process of reduction in 50 mM Tris buffer, 6 M urea, 30% glycerol, 2% SDS, followed by alkylation in buffer containing 2.5% of iodoacetamide (IAA), before the second dimension. Electrophoresis was performed in 25 cm × 21 cm × 1 mm homogeneous polyacrylamide 12.5% gels in two steps: i) 2 W/gel for 1 h and ii) 15 W/gel for 6 h.

### 2.6. Gel image analysis and differential spot selection

Gel scanning was carried out on a Typhoon™ 9400 Variable Mode scanner (Amersham Biosciences, Uppsala, Sweden). An image file analysis was performed with the DeCyder™ 6.0 Differential Analysis software (Amersham Biosciences, Uppsala, Sweden), which obtains data on protein levels with statistically significant differences. Interferences were manually minimized and the differentially accumulated spots were selected using a Student t-Test (*p*-value ≤ 0.05) and False Discovery Rate (FDR), in order to prevent false positives.

### 2.7. Differential spot identification and annotation

Selected spots were manually excised from gels and digested with trypsin. LC MS/MS spectra and MS/MS were obtained in an Autoflex III

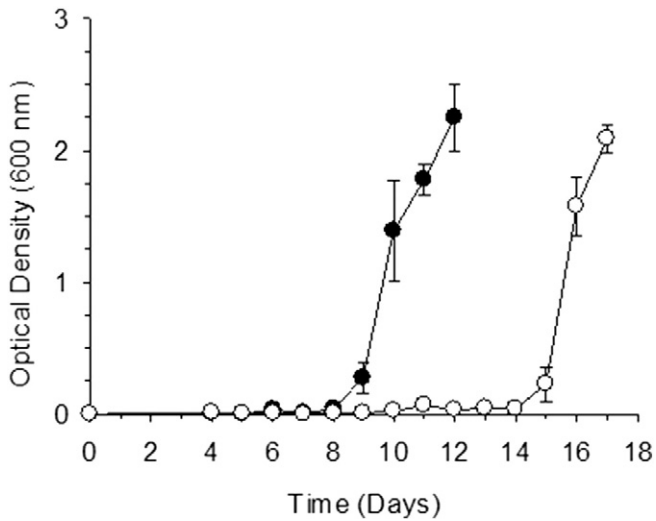


**Fig. 1.** Growth curves of *B. bruxellensis* cells in synthetic wine with 100 mg/L of *p*-coumaric acid.

MALDI-ToF/ToF spectrometer. Spectra were putatively identified by using local ascot software methods of peptide mass fingerprinting for MS data and ion search for MS/MS data, against *B. bruxellensis* AWRI\_1499 protein database obtained from NCBI and UniProt. Putative annotated protein sequences were retrieved in FASTA format and grouped by molecular function and biological process Clusters of Orthologous Groups (COGs).

### 3. Results

#### 3.1. Profile yeast growth in the presence of *p*-coumaric acid

As expected, the growth assays showed that the wine strain *B. bruxellensis* LAMAP2480 grew with a significant delay (over 7 d) in the presence of *p*-coumaric acid. This was despite yeast growth in the presence of acid reaching similar values to the control treatment (Fig. 1). A normal consumption of glucose was observed in both conditions (data not shown). Samples were taken when the cultures reached a similar exponential growth phase, to avoid any variability in the comparative proteomic analysis.

#### 3.2. Proteomic analysis

To identify proteomic changes caused by the presence of *p*-coumaric acid, protein extracts were separated by 2D electrophoresis. A total of six protein samples were analyzed for each treatment: with or without *p*-coumaric acid. On average, the comparative analysis of 2D electrophoresis gel images provided the detection of 925 differentially expressed proteins (Fig. 2). During the analysis with DeCyder™ Differential Analysis software, spots with quantitative changes ( $p$ -value  $\leq 0.001$ ) were considered. Based on this analysis, a total of 179 proteins showed significant changes in abundance under the different treatments. Finally, in order to narrow the data, a new selection was performed by applying a 99.99% confidence level ( $p$ -value  $\leq 0.0001$ ) and an abundance of  $\geq 2$ . Under these conditions, a total of 41 proteins were detected and selected to be identified (Table 1). The analysis of proteins from the total proteins accumulated differentially in the presence of *p*-coumaric acid revealed that the majority showed an upregulated accumulation with a fold change variation between 2.02 and 9.79 (Table 1). Interestingly, only one protein identified as a phosphoglycerate mutase (spot 2206), involved in the glycolysis pathway displayed a downregulation in the presence of *p*-coumaric acid; all other proteins upregulated (Table 1).

#### 3.3. Analysis of differentially accumulated proteins

The sequence homology analysis was performed using the *B. bruxellensis* AWRI1499 (Australian strain) databases available, which were then compared with genomic data of the Chilean strain LAMAP2480. The 41 differentially accumulated and identified proteins were divided into different categories according to biological processes and molecular function by COGs. It can be observed that the proteins are clustered in three biological processes: (A) metabolism, (B) cellular processes and signaling and, (C) information storage and processing (Fig. 3). Moreover, the functional category distribution for molecular processes showed that the addition of *p*-coumaric acid led to the accumulation of proteins belonging to the category of 'translational, ribosomal structure and biogenesis' (26.7%) and 'post-translational modification, protein turnover and chaperones' (20.6%) (Fig. 4). Interestingly, the third and fourth main group of this distribution was 'energy production and conversion' and 'amino acid transport and metabolism', which include 14.7% and 8.8% of the total

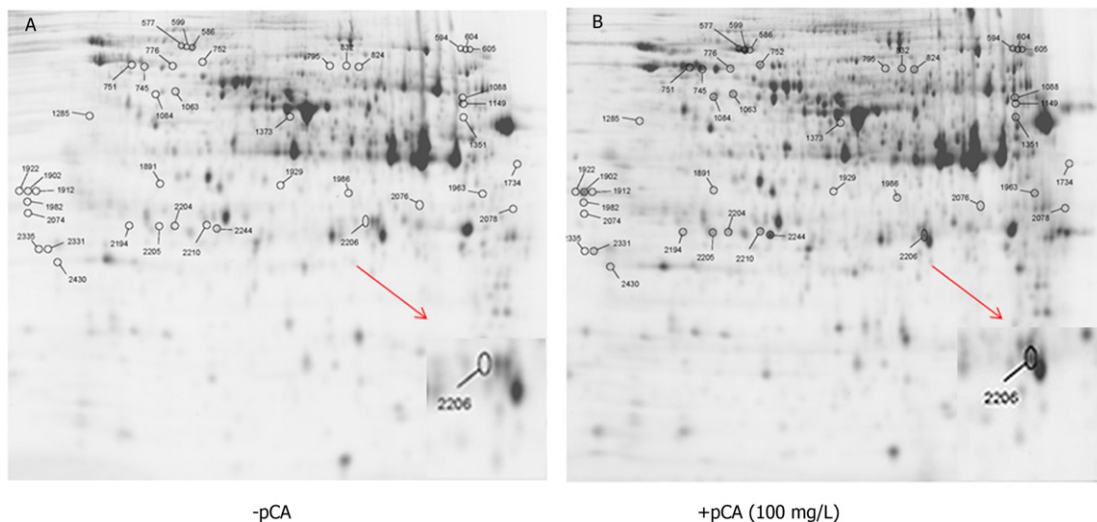


**Fig. 2.** Differentially accumulated proteins detected in 2D-PAGE. 2D-gel showing proteome profile of *B. bruxellensis* cells and numbered spots corresponding to the proteins identified during growth in synthetic wine without (A) and with (B) 100 mg/L of *p*-coumaric acid.

**Table 1**  
Proteins of *Brettanomyces bruxellensis* differentially accumulated during growth in synthetic wine with 100 mg/L of *p*-coumaric acid. Numbered spots correspond to proteins observed in Fig. 2.

| Ot   | NCBI Acc. no. <i>D. bruxellensis</i> AWRI1499 | % seq. Cov. | Acc. UniProt | Protein description blast <i>D. bruxellensis</i> AWRI1499 | Fold change | Acc. no. <i>D. bruxellensis</i> LAMAP2480 | Score bits | E value  | Identity (%) | Protein description blast <i>D. bruxellensis</i> LAMAP2480         |
|------|---|-------------|--------------|---|-------------|---|------------|----------|--------------|--|
| 577  | gi 385,303,999                                | 25          | I2JY15       | Heat shock protein Hsp88                                  | 3,67        | DEB_0656                                  | 1097       | 0        | 98           | Heat shock protein homolog Sse1                                    |
| 586  | gi 385,303,999                                | 26          | I2JY15       | Heat shock protein Hsp88                                  | 3,16        | DEB_0656                                  | 1097       | 0        | 98           | Heat shock protein homolog Sse1                                    |
| 594  | gi 385,304,066                                | 17          | I2JYP9       | Translation initiation factor eIF3 subunit                | 2,46        | DEB_5225                                  | 1393       | 0        | 95           | eIF3b subunit of the core complex of translation eIF3              |
| 599  | gi 385,303,999                                | 24          | I2JY15       | Heat shock protein Hsp88                                  | 3,01        | DEB_0656                                  | 1097       | 0        | 98           | Heat shock protein homolog Sse1                                    |
| 604  | gi 385,304,182                                | 15          | I2JZ09       | Glutamyl-tRNA synthetase                                  | 2,29        | DEB_3410                                  | 1329       | 0        | 94           | Glutamyl-tRNA synthetase (GluRS)                                   |
| 605  | gi 385,303,590                                | 9           | I2JXF2       | Aconitase mitochondrial precursor                         | 2,46        | DEB_2803                                  | 1533       | 0        | 97           | Aconitase  |
| 745  | gi 385,303,397                                | 15          | I2JWX0       | Heat shock protein Ssb1                                   | 3,35        | DEB_0154                                  | 1167       | 0        | 94           | Cytoplasmic ATPase   |
| 751  | gi 385,303,397                                | 38          | I2JWX0       | Heat shock protein Ssb1                                   | 3,42        | DEB_0154                                  | 1167       | 0        | 94           | Ribosome-associated molecular chaperone<br>Cytoplasmic ATPase      |
| 752  | gi 385,304,308                                | 13          | I2JZC9       | Mitochondrial matrix ATPase                               | 2,02        | DEB_3227                                  | 1192       | 0        | 93           | Ribosome-associated molecular chaperone<br>Hsp70 family ATPase     |
| 776  | gi 385,303,397                                | 16          | I2JWX0       | Heat shock protein Ssb1                                   | 2,17        | DEB_0154                                  | 1167       | 0        | 94           | Cytoplasmic ATPase: Ribosome-associated molecular chaperone        |
| 795  | gi 385,305,672                                | 11          | I2K328       | Polyadenylate-binding protein                             | 2,24        | DEB_6112                                  | 1226       | 0        | 90           | Poly(A) binding protein  |
| 824  | gi 385,305,672                                | 23          | I2K328       | Polyadenylate-binding protein                             | 2,36        | DEB_6112                                  | 1226       | 0        | 90           | Poly(A) binding protein  |
| 832  | gi 385,305,672                                | 11          | I2K328       | Polyadenylate-binding protein                             | 2,52        | DEB_6112                                  | 1226       | 0        | 90           | Poly(A) binding protein  |
| 1063 | gi 385,302,952                                | 28          | I2JVQ3       | Vacuolar ATP synthase subunit b                           | 2,04        | DEB_8230                                  | 903        | 0        | 100          | Subunit B of the vacuolar H <sup>+</sup> -ATPase (V-ATPase)        |
| 1084 | gi 385,302,952                                | 25          | I2JVQ3       | Vacuolar ATP synthase subunit b                           | 3,85        | DEB_8230                                  | 903        | 0        | 100          | Subunit B of the vacuolar H <sup>+</sup> -ATPase (V-ATPase)        |
| 1088 | gi 385,303,472                                | 19          | I2JX43       | Delta-1-pyrroline-5-carboxylate dehydrogenase             | 2,52        | DEB_1480                                  | 1069       | 0        | 99           | Delta-1-pyrroline-5-carboxylate dehydrogenase                      |
| 1149 | gi 385,305,298                                | 15          | I2K234       | Serine mitochondrial precursor                            | 2,02        | DEB_0153                                  | 841        | 0        | 86           | Mitochondrial serine hydroxymethyltransferase                      |
| 1285 | gi 385,303,397                                | 22          | I2JWX0       | Heat shock protein Ssb1                                   | 2,05        | DEB_0154                                  | 1167       | 0        | 94           | Cytoplasmic ATPase.<br>Ribosome-associated molecular chaperone     |
| 1351 | gi 385,301,161                                | 49          | I2JQX1       | Isocitrate mitochondrial precursor                        | 3,18        | DEB_9391                                  | 914        | 0        | 97           | Mitochondrial NADP <sup>+</sup> -specific isocitrate dehydrogenase |
| 1373 | gi 385,301,947                                | 10          | I2JT02       | Translation elongation factor 2                           | 2,06        | DEB_5012                                  | 1523       | 0        | 96           | Elongation factor 2 (EF-2)   |
| 1734 | gi 385,304,846                                | 6           | I2K0U7       | Malate NAD <sup>+</sup> -dependent                        | 2,05        | DEB_6563                                  | 659        | 0        | 99           | Mitochondrial malate dehydrogenase                                 |
| 1891 | gi 385,303,892                                | 22          | I2JY86       | Sphingolipid long chain base-responsive protein Pil1      | 2,33        | DEB_9433                                  | 466        | e-132    | 83           | Primary component of eisosomes                                     |
| 1902 | gi 385,304,034                                | 13          | I2JYL8       | Elongation factor 1-β                                     | 9,79        | DEB_5213                                  | 235        | 6,00E-63 | 64           | Elongation factor 1-β  |
| 1912 | gi 385,304,034                                | 3           | I2JYL8       | Elongation factor 1-β                                     | 8,12        | DEB_5213                                  | 235        | 6E-63    | 64           | Elongation factor 1-β  |
| 1922 | gi 385,306,057                                | 6           | I2K441       | 60s ribosomal protein l8-b                                | 6,89        | DEB_7740                                  | 472        | e-134    | 90           | Ribosomal protein L4 of the large (60S) ribosomal subunit          |
| 1929 | gi 385,305,338                                | 2           | I2K272       | 40s ribosomal protein s5                                  | 2,41        | DEB_3786                                  | 423        | e-129    | 100          | Protein component of the small (40S) ribosomal subunit             |
| 1973 | gi 385,301,952                                |             | I2JT04       | YMR226c-like protein                                      | 2,25        | DEB_3523                                  | 534        | e-153    | 98           | NADP <sup>+</sup> -dependent dehydrogenase                         |
| 1982 | gi 385,306,057                                | 9           | I2K441       | 60s ribosomal protein l8-b                                | 5,71        | DEB_7740                                  | 472        | e-134    | 90           | Ribosomal protein L4 of the large (60S) ribosomal subunit          |
| 1986 | gi 385,303,283                                | 28          | I2JWL7       | Sphingolipid long chain base-responsive protein Pil1      | 2,36        | DEB_9433                                  | 395        | e-111    | 74           | Primary component of eisosomes                                     |
| 2074 | gi 385,306,053                                | 4           | I2K437       | 60s ribosomal protein l2                                  | 4,43        | DEB_7737                                  | 484        | e-137    | 94           | Protein component of the large (60S) ribosomal subunit             |
| 2076 | gi 385,301,733                                | 14          | I2JSF0       | Alcohol dehydrogenase                                     | 2,15        | DEB_7598                                  | 453        | e-128    | 64           | Mitochondrial alcohol dehydrogenase                                |
| 2078 | gi 385,303,430                                | 2           | I2JX01       | Glyceraldehyde-3-phosphate dehydrogenase                  | 5,38        | DEB_4294                                  | 674        | 0        | 98           | Glyceraldehyde-3-phosphate dehydrogenase                           |
| 2194 | gi 385,305,335                                | 3           | I2K269       | Heat shock protein Hsp20                                  | 3,74        | DEB_3791                                  | 364        | e-101    | 89           | Small heat shock protein C4  |
| 2204 | gi 385,304,076                                | 17          | I2JYQ7       | Mitochondrial peroxiredoxin Prx1                          | 2,99        | DEB_0579                                  | 471        | e-134    | 99           | Mitochondrial peroxiredoxin  |
| 2205 | gi 385,305,335                                | 5           | I2K269       | Heat shock protein Hsp20                                  | 3,47        | DEB_3791                                  | 364        | e-101    | 89           | Small heat shock protein C4  |
| 2206 | gi 385,300,983                                | 13          | I2JQG8       | Phosphoglycerate mutase                                   | -2,11       | DEB_6902                                  | 483        | e-137    | 95           | Tetrameric phosphoglycerate mutase                                 |
| 2210 | gi 385,305,359                                | 27          | I2K291       | Vacuolar ATP synthase subunit E                           | 5,95        | DEB_11809                                 | 350        | 2,00E-97 | 93           | Subunit E of the vacuolar H <sup>+</sup> -ATPase (V-ATPase)        |
| 2244 | gi 385,304,076                                | 11          | I2JYQ7       | Mitochondrial peroxiredoxin Prx1                          | 3,82        | DEB_0579                                  | 471        | e-134    | 99           | Mitochondrial peroxiredoxin  |
| 2331 | gi 385,303,768                                | 3           | I2JXW9       | Translationally controlled tumor protein                  | 2,44        | DEB_9730                                  | 320        | 1,00E-88 | 93           | Protein that associates with ribosomes                             |
| 2335 | gi 385,305,439                                | 4           | I2K2G2       | Eukaryotic translation initiation factor 5a               | 2,46        | DEB_1606                                  | 313        | 1,00E-86 | 99           | Translation elongation factor eIF-5 A                              |
| 2430 | gi 385,303,843                                | 6           | I2JY42       | Peroxioredoxin Tsa1                                       | 4,02        | DEB_7532                                  | 404        | e-113    | 100          | Thioredoxin peroxidase   |

proteins, respectively. These latter groups can be related to energetic imbalance that supposes the maintenance of intracellular pH.

#### 4. Discussion

In this study, we carried out an analysis of the proteome changes occurring in yeast during the exponential growth phase, in the presence of *p*-coumaric acid. Within the cells exposed to *p*-coumaric

acid, we detected an increased accumulation of proteins related to stress proteins and chaperones such as Hsp20, 88 and several Hsp70 isoforms. The small heat shock proteins (sHSP) have been described in different tissues and organisms only in stress conditions [22]. They are induced by exposure to a range of stress factors, such as Hsp26, which is induced by osmolarity [23], heat shock [24], H<sub>2</sub>O<sub>2</sub> [25] or exposure to sorbic acid [26]. Hsp20 (spots 2194 and 2205), is a well characterized protein in plants and is induced by heat-stress [22]. In

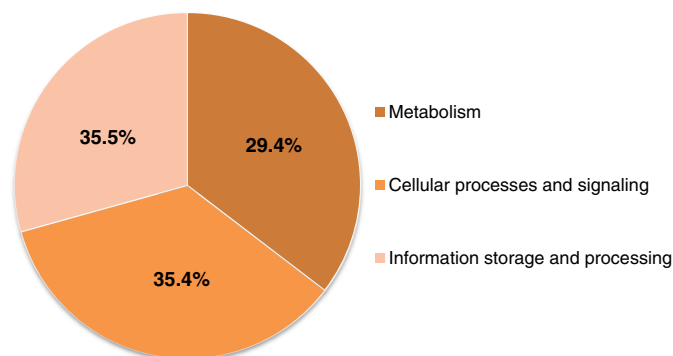


Fig. 3. Functional category distribution of identified differential proteins associated by Clusters of Orthologous Groups for biological processes.

stress conditions, Hsp20 aggregate to form complexes such as intracellular matrices to prevent protein denaturation [27]. However, the precise role and function of Hsp20 under weak acid stress in yeast remains unknown. In *Saccharomyces cerevisiae*, it has been proposed that Hsp26 could be used to prepare denatured proteins for refolding or degradation under sorbic acid stress [26]. In our case, Hsp20 could exert a similar role in the resistance to *p*-coumaric acid. In this regard, the data suggests that an inhibitory action of *p*-coumaric acid could be intracellular protein denaturation, as has been described for sorbic acid [26]. In this context, other HSP were also induced under *p*-coumaric acid stress, such as Hsp70 isoforms (spots 745, 751, 776 and 1285). Hsp70 are specialized proteins involved in translation and early polypeptide folding processes [28]. It is known that Ssb1 (Hsp70) is induced by H<sub>2</sub>O<sub>2</sub> [25] in response to sorbic acid [26] and its deletion produces mutants which are more sensitive to low temperatures and salt [29]. Furthermore, we observed the accumulation of Hsp88 isoforms (spots 577, 586 and 599) or Sse1p in synthetic wine in the presence of ethanol. Previous works have described Sse1p as proteins involved in environmental stress responses, which are accumulated in the presence of ethanol, and prevent protein unfolding [30]. The increase of these proteins in the presence of *p*-coumaric acid could be indicative of an increase in damaged intracellular proteins or a major protein expression and/or turnover in *p*-coumaric acid stress.

Several ribosomal proteins (spots 1922, 1924, 2074) and translation elongation factors (spots 1373, 1912), along with different translation initiation factors (spots 594, 2335) (Table 1), show a greater accumulation under *p*-coumaric acid conditions, suggesting that the synthesis of most general proteins is activated under these conditions. Translation elongation factors such as EF-3A, similar to the ones

detected in this work, have been described in *S. cerevisiae* under sorbic acid stress conditions [26]. Studies on the adaptive response to acetic acid in the highly resistant yeast *Zygosaccharomyces bailii*, have shown an increased accumulation of the translation initiation factor eIF-5A and protein component of the small (40S) ribosomal subunit [31], similar to the proteins detected in *B. bruxellensis* in the presence of the weak *p*-coumaric acid [31]. The accumulation of these proteins, in association with the overproduction of chaperones, may stimulate protein synthesis rate for the cells to grow even under unfavorable conditions of *p*-coumaric acid. In fact, the data suggests the synthesis of most proteins activated by *p*-coumaric acid is to restructure the mechanism for more energy production (see below).

Metabolism was the principal biological process determined in this study (Fig. 3), energy production and conversions were included as the principal molecular functions (Table 1). This category can be related to an energetic imbalance that supposes the maintenance of intracellular pH under weak acid conditions. The dissociation of weak acids in the cell leads to the accumulation of protons and of the corresponding anions resulting in internal acidification [32]. Hydroxycinnamic acids diffuse into the cell affecting cellular pH, blocking transport and inhibiting growth [5]. To counteract the weak acid induced intracellular acidification, an increase in the activity of the plasma membrane H<sup>+</sup>-ATPase and of the vacuolar ATP synthase (V-ATPase) is observed under weak acid stress [32]. An H<sup>+</sup>-ATPase pump which supports a mechanism to counteract the decrease in internal pH caused by the presence of this acid, has been described in *B. bruxellensis* in response to *p*-coumaric acid growth [8]. Two different V-ATPase subunits were spotted in our study (spots 1063, 1084 and 2210), both included in the molecular category energy production and conversion (Fig. 4). V-ATPases are large, complex enzymes responsible for the translocation of protons into the lumen from the cytoplasm. This action is very important for many cellular processes, such as endocytosis, cytoplasmic pH homeostasis, protein processing, and the coupled transport of small molecules. Moreover, it plays an important role in stress tolerance [33,34]. These data suggest a role for V-ATPases in tolerance to *p*-coumaric acid maintaining cytoplasmic pH homeostasis. Additionally, the treatments with sorbic acid in *S. cerevisiae* promoted the accumulation of Atp2, a mitochondrial ATPase  $\beta$ -subunit [26]. The apparent increase of energy generation during adaptation to *p*-coumaric acid growth is supported by previous investigations, which show the excess consumption of intracellular ATP pools as an attempt to restore the homeostasis under weak acid conditions [35,36]. Interestingly, different works have shown the upregulation of Atp2 by ethanol [37]. In our study *B. bruxellensis* was grown in SW containing 10% ethanol, which could be contributing to the accumulation of V-ATPases observed.

In addition to the accumulation of mitochondrial proteins involved in energy generation, we also detected three proteins that belong to

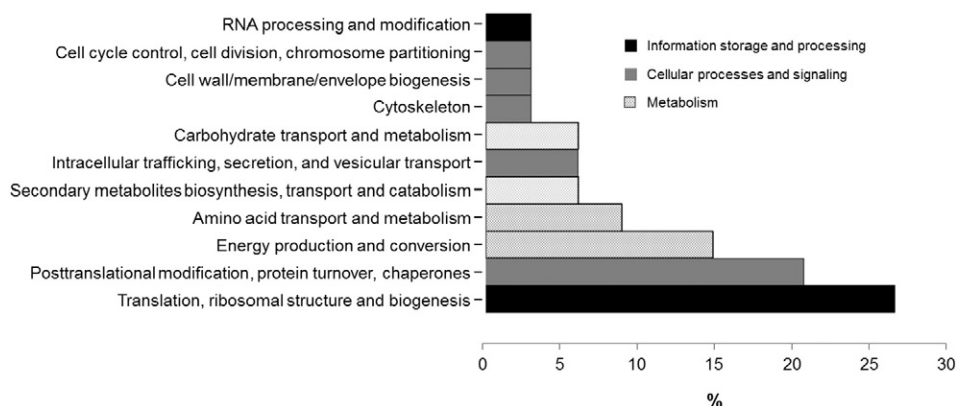


Fig. 4. Functional category distribution of identified differential proteins associated by Clusters of Orthologous Groups for molecular function.

the tricarboxylic acid cycle (TCA): aconitase (spot 605), malate dehydrogenase (spot 1734) and NADP<sup>+</sup>-specific dehydrogenase (spot 1351). The stimulation of TCA flux in *p*-coumaric acid stressed *B. bruxellensis* cells allows the enhancement of the ATP pool. Previously, malate dehydrogenase has been found to be required for the first step of weak acid metabolism in the resistant yeast *Z. bailii* [31,38]. This yeast is resistant to acetate and has the ability to metabolize the acid in the presence of glucose, while in similar conditions malate dehydrogenase was depressed in *S. cerevisiae*. Considering this data, the increase of this enzyme in *B. bruxellensis* is consistent with the high accumulation of V-ATPases, due to an increase of ATP synthesis required in the presence of weak acids. This supports the energy-consuming mechanism necessary to counteract its deleterious action, as has been reported in *S. cerevisiae* [31,32,39,40].

In relation to energy generation, other enzymes belonging to the dehydrogenase family have been detected during growth of *B. bruxellensis* under *p*-coumaric acid stress (spots 1973, 2076 and 2078). In *S. cerevisiae* these enzymes form complexes in the mitochondria. One of these complexes has three NADH-dehydrogenases, a glycerol-3-phosphate dehydrogenase, an acetaldehyde dehydrogenase and TCA enzymes (malate dehydrogenase, citrate synthase, succinate dehydrogenase and fumarate hydratase) [41]. In our work, a variety of these enzymes have been detected, suggesting an increase of NADH and ATP pools, which corroborate the resulting high energy demand for growth under *p*-coumaric acid conditions. These assumptions are in agreement with the increased accumulation of glyceraldehyde-3-phosphate dehydrogenase (spot 2078) (Table 1), a glycolytic enzyme responsible for formation of 1,3-bisphosphoglycerate and NADH. Furthermore, an alcohol dehydrogenase (spot 2076) (Table 1) was present in our study under *p*-coumaric acid conditions. This fact may be related to an increase of glycolytic flux through glucose to compensate for the energetic imbalance caused by the weak acid. Other works described evidence of an enhancement of the key glycolytic enzymes [26], which support previous observations stressing the importance of an energy-generating metabolism to weak acid adaptation [35,36]. Moreover, in previous studies with nitrate, *B. bruxellensis* presented a metabolic flux regulation, with an increase of ATP synthesis, TCA and glycolytic enzymes and an overproduction of alcohol dehydrogenase in order to compensate for the energetic imbalance caused by nitrate assimilation [42]. These data suggest that *B. bruxellensis* could present similar behavior in the presence of *p*-coumaric acid, which induces the same metabolic responses in order to obtain the necessary energy to cover the energetic demand caused by growing under these stress conditions. On the other hand, the only enzyme not accumulated was a phosphoglycerate mutase (spot 2206) (Table 1) responsible for the conversion of 3-phosphoglycerate to 2-phosphoglycerate.

In this work we detected an increased accumulation of the  $\Delta^1$ -pyrroline-5-carboxylate dehydrogenase (spot 1088) in *B. bruxellensis* under *p*-coumaric acid stress. Structurally, this enzyme has been well characterized in *S. cerevisiae* [41,43] and is involved in the conversion of the excess proline to glutamate in the mitochondria [44]. Proline catabolism intermediate  $\Delta^1$ -pyrroline-5-carboxylate is toxic to yeast cells because of the formation of ROS [45] and directly inhibits mitochondrial respiration [46]. This compound is metabolized by  $\Delta^1$ -pyrroline-5-carboxylate dehydrogenase into a non-toxic intermediate, the amino acid glutamate [43,45,46]. Moreover, the enzyme is required in different species to regulate redox state, homeostasis and virulence [47,48]. Even in plants, it has been described as playing an important role in protection from proline metabolism toxicity [49]. On the other hand, it has been described that proline-accumulating strains displayed tolerance to acetic acid, whereas strains with compromised proline metabolism displayed sensitivity [50]. Furthermore, sensitivity to weak acids appears to be reduced with the addition of proline. The data suggests that the increased accumulation of  $\Delta^1$ -pyrroline-5-carboxylate dehydrogenase

for glutamate formation could be a strategy of *B. bruxellensis* to obtain precursors for TCA and an increase of ATP, in order to equilibrate the homeostasis in *p*-coumaric acid conditions. In our study, a mitochondrial peroxiredoxin Prd1 (spots 2204 and 2244) and a peroxiredoxin Tsa1 (spots 2430) were accumulated during stress conditions (Table 1). The first presented thioredoxin peroxidase activity and is induced during respiratory growth and oxidative stress [51]. The second, considered as the major yeast peroxiredoxin, acts as both a ribosome-associate and a free cytoplasmic antioxidant. It functions as a specific antioxidant in the cytoplasm to protect the cell against the oxidative stress caused by nascent-protein misfolding and aggregation [52]. Transcript analysis carried out in *S. cerevisiae* grown in sorbic acid displayed many enzymes involved in reducing oxidative stress, which were not detected in the proteomic study. However, our work revealed different proteins related with these processes and apparently induced by *p*-coumaric acid stress.

Within the differentially accumulated proteins, it was not possible to find Pad1p, enzyme responsible for decarboxylating *p*-coumaric acid and converting it into 4-vinylphenol [20]. It has been reported that 4-ethylphenol formation is growth associated, and occurs roughly between mid-exponential growth phase and the beginning of the stationary phase [53]. This could explain the absence of the Pad1 protein within the differentially accumulated proteins, therefore, this enzyme decarboxylated the *p*-coumaric acid in the early stages of growth. Our results show proteins accumulated during the exponential phase, wherein the second reaction step occurs, corresponding to the reduction of 4-vinylphenol to 4-ethylphenol.

In this work we have explored 2DE-based expression proteomics focusing on the growth of *B. bruxellensis* LAMAP2480 in the presence of hydroxycinnamic acids namely *p*-coumaric acid, to extend the knowledge on the mechanisms underlying its response to weak acid. The results indicate that the response to *p*-coumaric acid involves an increased activity of different metabolic processes to improve the requirements of ATP and NADH production, in order to assure cell detoxification. Results also suggest that there is an induction of protective mechanisms in response to the acid, in particular, through the induction of RNA machinery, oxidative stress response and an increase of TCA flux. Taken together, data obtained from this study provides insights into *p*-coumaric acid adaptation in the wine spoilage yeast *B. bruxellensis*.

## Conflict of interests

The authors declare that they have no competing interests.

## Financial support

This work was developed as part of the following research network: grant DICYT-USACH (DICYT-081471CL), grant from the National Fund for Scientific and Technological Development (FONDECYT-1110700), Millennium Nucleus for Fungal Integrative and Synthetic Biology (MN-FISB) 120043 grant and CONICYT Postdoctorado/FONDECYT 3140083.

## References

- [1] Benito S, Palomero F, Morata A, Calderón F, Suárez-Lepe JA. Factors affecting the hydroxycinnamate decarboxylase/vinylphenol reductase activity of *Dekkera/Brettanomyces*: Application for *Dekkera/Brettanomyces* control in red wine making. *J Food Sci* 2009;74:15–22. <http://dx.doi.org/10.1111/j.1750-3841.2008.00977.x>.
- [2] De Souza Liberal AT, Basílio ACM, Do Monte Resende A, Brasileiro BTV, Da Silva-Filho EA, De Morais JOF, et al. Identification of *Dekkera bruxellensis* as a major contaminant yeast in continuous fuel ethanol fermentation. *J Appl Microbiol* 2007;102:538–47. <http://dx.doi.org/10.1111/j.1365-2672.2006.03082.x>.
- [3] Godoy L, Garrido D, Martínez C, Saavedra J, Combina M, Ganga M. Study of the coumarate decarboxylase and vinylphenol reductase activities of *Dekkera bruxellensis* (anamorph *Brettanomyces bruxellensis*) isolates. *Lett Appl Microbiol* 2009;48:452–7. <http://dx.doi.org/10.1111/j.1472-765X.2009.02556.x>.

- [4] Maksymowych WP, Suarez-Almazor ME, Buenviaje H, Cooper BL, Degeus C, Thompson M, et al. HLA and cytokine gene polymorphisms in relation to occurrence of palindromic rheumatism and its progression to rheumatoid arthritis. *J Rheumatol* 2002;29:2319–26.
- [5] Piper P, Ortiz Calderon C, Hatzixanthos K, Mollapour M. Weak acid adaptation : The stress response that confers yeasts with resistance to organic acid food preservatives. *Microbiology* 2001;147:2635–42. <http://dx.doi.org/10.1099/0021287-147-10-2635>.
- [6] Harris V, Jiranek V, Ford CM, Grbin PR. Inhibitory effect of hydroxycinnamic acids on *Dekkera* spp. *Appl Microbiol Biotechnol* 2010;86:721–9. <http://dx.doi.org/10.1007/s00253-009-2352-6>.
- [7] Stratford M, Nebe-von-Caron G, Steels H, Novodvorska M, Ueckert J, Archer DB. Weak-acid preservatives: pH and proton movements in the yeast *Saccharomyces cerevisiae*. *Int J Food Microbiol* 2013;161:164–71. <http://dx.doi.org/10.1016/j.jfoodmicro.2012.12.013>.
- [8] Godoy L, Varela J, Martínez C, Ganga CM, et al. The effect of hydroxycinnamic acids on growth and H<sup>+</sup>-ATPase activity of the wine spoilage yeast, *Dekkera bruxellensis*. *African J Microbiol Res* 2013;7:5300–5. <http://dx.doi.org/10.5897/AJMR2013.6350>.
- [9] Conterno L, Joseph CML, Arvik TJ, Henick-Kling T, Bisson LF. Genetic and physiological characterization of *Brettanomyces bruxellensis* strains isolated from wines. *Am J Enol Vitic* 2006;57:139–47.
- [10] Fariña L, Boido E, Carrau F, Dellacassa E. Determination of volatile phenols in red wines by dispersive liquid–liquid microextraction and gas chromatography–mass spectrometry detection. *J Chromatogr A* 2007;1157:46–50. <http://dx.doi.org/10.1016/j.chroma.2007.05.006>.
- [11] Hellborg L, Piskur J. Complex nature of the genome in a wine spoilage yeast, *Dekkera bruxellensis*. *Eukaryot Cell* 2009;8:1739–49. <http://dx.doi.org/10.1128/EC.00115-09>.
- [12] Woolfit M, Rozpedowska E, Piskur J, Wolfe KH. Genome survey sequencing of the wine spoilage yeast *Dekkera (Brettanomyces) bruxellensis*. *Eukaryot Cell* 2007;6:721–33. <http://dx.doi.org/10.1128/EC.00338-06>.
- [13] Vigentini I, Lucy Joseph CM, Picozzi C, Foschino R, Bisson LF. Assessment of the *Brettanomyces bruxellensis* metabolome during sulphur dioxide exposure. *FEMS Yeast Res* 2013;13:597–608. <http://dx.doi.org/10.1111/1567-1364.12060>.
- [14] Borneman AR, Zeppel R, Chambers PJ, Curtin CD. Insights into the *Dekkera bruxellensis* genomic landscape: Comparative genomics reveals variations in ploidy and nutrient utilisation potential amongst wine isolates. *PLoS Genet* 2014;10:e1004161. <http://dx.doi.org/10.1371/journal.pgen.1004161>.
- [15] Curtin CD, Pretorius IS. Genomic insights into the evolution of industrial yeast species *Brettanomyces bruxellensis*. *FEMS Yeast Res* 2014;14:997–1005. <http://dx.doi.org/10.1111/1567-1364.12198>.
- [16] Agnolucci M, Vigentini I, Capurso G, Merico A, Tirelli A, Compagno C, et al. Genetic diversity and physiological traits of *Brettanomyces bruxellensis* strains isolated from Tuscan Sangiovese wines. *Int J Food Microbiol* 2009;130:238–44. <http://dx.doi.org/10.1016/j.jfoodmicro.2009.01.025>.
- [17] Coronado P, Aguilera S, Carmona L, Godoy L, Martínez C, Ganga MA. Comparison of the behaviour of *Brettanomyces bruxellensis* strain LAMAP L2480 growing in authentic and synthetic wines. *Antonie Van Leeuwenhoek* 2015;107:1217–23. <http://dx.doi.org/10.1007/s10482-015-0413-7>.
- [18] Valdes J, Tapia P, Cepeda V, Varela J, Godoy L, Cubillos FA, et al. Draft genome sequence and transcriptome analysis of the wine spoilage yeast *Dekkera bruxellensis* LAMAP2480 provides insights into genetic diversity, metabolism and survival. *FEMS Microbiol Lett* 2014;361:104–6. <http://dx.doi.org/10.1111/1574-6968.12630>.
- [19] Sturm ME, Arroyo-López FN, Garrido-Fernández A, Querol A, Mercado LA, Ramirez ML, et al. Probabilistic model for the spoilage wine yeast *Dekkera bruxellensis* as a function of pH, ethanol and free SO<sub>2</sub> using time as a dummy variable. *Int J Food Microbiol* 2014;170:83–90. <http://dx.doi.org/10.1016/j.jfoodmicro.2013.10.019>.
- [20] Godoy L, Martínez C, Carrasco N, Ganga MA. Purification and characterization of a p-coumarate decarboxylase and a vinylphenol reductase from *Brettanomyces bruxellensis*. *Int J Food Microbiol* 2008;127:6–11. <http://dx.doi.org/10.1016/j.jfoodmicro.2008.05.011>.
- [21] Bradford MM. A rapid and sensitive method for the quantitation of microgram quantities of protein utilizing the principle of protein–dye binding. *Anal Biochem* 1976;72:248–54. [http://dx.doi.org/10.1016/0003-2697\(76\)90527-3](http://dx.doi.org/10.1016/0003-2697(76)90527-3).
- [22] Kirschner M, Winkelhaus S, Thierfelder JM, Nover L. Transient expression and heat-stress-induced co-aggregation of endogenous and heterologous small heat-stress proteins in tobacco protoplasts. *Plant J* 2000;24:397–411. <http://dx.doi.org/10.1046/j.1365-3113x.2000.00887.x>.
- [23] Blomberg A. Osmoresponsive proteins and functional assessment strategies in *Saccharomyces cerevisiae*. *Electrophoresis* 1997;18:1429–40. <http://dx.doi.org/10.1002/elps.1150180818>.
- [24] Roth FP, Hughes JD, Estep PW, Church GM. Finding DNA regulatory motifs within unaligned noncoding sequences clustered by whole-genome mRNA quantitation. *Nat Biotechnol* 1998;16:939–45. <http://dx.doi.org/10.1038/nbt1098-939>.
- [25] Godon C, Lagniel G, Lee J, Buhler JM, Kieffer S, Perrot M, et al. The H<sub>2</sub>O<sub>2</sub> stimulant in *Saccharomyces cerevisiae*. *J Biol Chem* 1998;273:22480–9. <http://dx.doi.org/10.1074/jbc.273.35.22480>.
- [26] De Nobel H, Lawrie L, Brul S, Klis F, Davis M, Allouh H, et al. Parallel and comparative analysis of the proteome and transcriptome of sorbic acid-stressed *Saccharomyces cerevisiae*. *Yeast* 2001;18:1413–28. <http://dx.doi.org/10.1002/yea.793>.
- [27] Kimpel JA, Key JL. Heat shock in plants. *Trends Biochem Sci* 1985;10:353–7. [http://dx.doi.org/10.1016/0968-0004\(85\)90111-2](http://dx.doi.org/10.1016/0968-0004(85)90111-2).
- [28] Conz C, Otto H, Peisker K, Gautschi M, Wölflle T, Mayer MP, et al. Functional characterization of the atypical Hsp70 subunit of yeast ribosome-associated complex. *J Biol Chem* 2007;282:33977–84. <http://dx.doi.org/10.1074/jbc.M706737200>.
- [29] Craig EA, Jacobsen K. Mutations in cognate genes of *Saccharomyces cerevisiae* hsp70 result in reduced growth rates at low temperatures. *Mol Cell Biol* 1985;5:3517–24. <http://dx.doi.org/10.1128/MCB.5.12.3517>.
- [30] Gasch AP, Spellman PT, Kao CM, Carmel-Harel O, Eisen MB, Storz G, et al. Genomic expression programs in the response of yeast cells to environmental changes. *Mol Cell Biol* 2000;20:4241–57. <http://dx.doi.org/10.1091/mbc.11.12.4241>.
- [31] Guerreiro JF, Mira NP, Sá-Correia I. Adaptive response to acetic acid in the highly resistant yeast species *Zygosaccharomyces bailii* revealed by quantitative proteomics. *Proteomics* 2012;12:2303–18. <http://dx.doi.org/10.1002/pmic.201100457>.
- [32] Mira NP, Teixeira MC, Sá-Correia I. Adaptive response and tolerance to weak acids in *Saccharomyces cerevisiae*: A genome-wide view. *OMICS J Integr Biol* 2010;14:525–40. <http://dx.doi.org/10.1002/omi.2010.0072>.
- [33] Hasegawa S, Ogata T, Tanaka K, Ando A, Takagi H, Shima J. Overexpression of vacuolar H<sup>+</sup>-ATPase-related genes in bottom-fermenting yeast enhances ethanol tolerance and fermentation rates during high-gravity fermentation. *J Inst Brew* 2012;118:179–85. <http://dx.doi.org/10.1002/jib.32>.
- [34] Makrantonou V, Dennison P, Stark MJR, Coote PJ. A novel role for the yeast protein kinase Dbf2p in vacuolar H<sup>+</sup>-ATPase function and sorbic acid stress tolerance. *Microbiology* 2007;153:4016–26. <http://dx.doi.org/10.1099/mic.0.2007/010298-0>.
- [35] Holyoak CD, Stratford M, McMullin Z, Cole MB, Crimmins K, Brown AJ, et al. Activity of the plasma membrane H<sup>+</sup>-ATPase and optimal glycolytic flux are required for rapid adaptation and growth of *Saccharomyces cerevisiae* in the presence of the weak-acid preservative sorbic acid. *Appl Environ Microbiol* 1996;62:3158–64. <http://dx.doi.org/10.1128/aem.62.10.3158-64.1996>.
- [36] Piper PW, Ortiz-Calderon C, Holyoak C, Coote P, Cole M. Hsp30, the integral plasma membrane heat shock protein of *Saccharomyces cerevisiae*, is a stress-inducible regulator of plasma membrane H<sup>+</sup>-ATPase. *Cell Stress Chaperones* 1997;2:12–24. [http://dx.doi.org/10.1379/1466-1268\(1997\)002<0012:htpmh>2.3.co;2](http://dx.doi.org/10.1379/1466-1268(1997)002<0012:htpmh>2.3.co;2).
- [37] Norbeck J, Blomberg A. Protein expression during exponential growth in 0.7 M NaCl medium of *Saccharomyces cerevisiae*. *FEMS Microbiol Lett* 1996;137:1–8. <http://dx.doi.org/10.1111/j.1574-6968.1996.tb08073.x>.
- [38] Sousa MJ, Rodrigues F, Córte-Real M, Leão C. Mechanisms underlying the transport and intracellular metabolism of acetic acid in the presence of glucose in the yeast *Zygosaccharomyces bailii*. *Microbiology* 1998;144:665–70. <http://dx.doi.org/10.1099/00221287-144-3-665>.
- [39] Mira NP, Palma M, Guerreiro JF, Sá-Correia I. Genome-wide identification of *Saccharomyces cerevisiae* genes required for tolerance to acetic acid. *Microb Cell Fact* 2010;9:79. <http://dx.doi.org/10.1186/1475-2859-9-79>.
- [40] Mira NP, Teixeira MC. Microbial mechanisms of tolerance to weak acid stress. *Front Microbiol* 2013;4:416. <http://dx.doi.org/10.3389/fmicb.2013.00416>.
- [41] Grandier-Vazeille X, Bathany K, Chaignepain S, Camougrand N, Manon S, Schmitter JM. Yeast mitochondrial dehydrogenases are associated in a supramolecular complex. *Biochemistry* 2001;40:9758–69. <http://dx.doi.org/10.1021/bi010277r>.
- [42] Neto AGB, Pestana-Calsa MC, de Moraes MA, Calsa T. Proteome responses to nitrate in bioethanol production contaminant *Dekkera bruxellensis*. *J Proteomics* 2014;104:104–11. <http://dx.doi.org/10.1016/j.jpro.2014.03.014>.
- [43] Pemberton TA, Srivastava D, Sanyal N, Henzl MT, Becker DF, Tanner JJ. Structural studies of yeast Δ(1)-pyrroline-5-carboxylate dehydrogenase (ALDH4A1): Active site flexibility and oligomeric state. *Biochemistry* 2014;53:1350–9. <http://dx.doi.org/10.1021/bi500048b>.
- [44] Takagi H. Proline as a stress protectant in yeast: Physiological functions, metabolic regulations, and biotechnological applications. *Appl Microbiol Biotechnol* 2008;81:211–23. <http://dx.doi.org/10.1007/s00253-008-1698-5>.
- [45] Nomura M, Takagi H. Role of the yeast acetyltransferase Mpr1 in oxidative stress: Regulation of oxygen reactive species caused by a toxic proline catabolism intermediate. *Proc Natl Acad Sci U S A* 2004;101:12616–21. <http://dx.doi.org/10.1073/pnas.0403349101>.
- [46] Nishimura A, Nasuno R, Takagi H. The proline metabolism intermediate Δ1-pyrroline-5-carboxylate directly inhibits the mitochondrial respiration in budding yeast. *FEMS Lett* 2012;586:2411–6. <http://dx.doi.org/10.1016/j.febslet.2012.05.056>.
- [47] Paes LS, Suárez Mantilla B, Zimbres FM, Pral EMF, Diogo de Melo P, Tahara EB, et al. Proline dehydrogenase regulates redox state and respiratory metabolism in *Trypanosoma cruzi*. *PLoS One* 2013;8:e69419. <http://dx.doi.org/10.1371/journal.pone.0069419>.
- [48] Lee IR, Lui EYL, Chow EWL, Arras SDM, Morrow CA, Fraser JA. Reactive oxygen species homeostasis and virulence of the fungal pathogen *Cryptococcus neoformans* requires an intact proline catabolism pathway. *Genetics* 2013;194:421–33. <http://dx.doi.org/10.1534/genetics.113.150326>.
- [49] Deuschle K, Funck D, Hellmann H, Däschner K, Binder S, Frommer WB. A nuclear gene encoding mitochondrial Delta-pyrroline-5-carboxylate dehydrogenase and its potential role in protection from proline toxicity. *Plant J* 2001;27:345–56. <http://dx.doi.org/10.1046/j.1365-3113x.2001.01101.x>.
- [50] Greetham D, Takagi H, Phister TP. Presence of proline has a protective effect on weak acid stressed *Saccharomyces cerevisiae*. *Antonie Van Leeuwenhoek* 2014;105:641–52. <http://dx.doi.org/10.1007/s10482-014-0118-3>.
- [51] Greetham D, Grant CM. Antioxidant activity of the yeast mitochondrial one-Cys peroxiredoxin is dependent on thioredoxin reductase and glutathione *in vivo*. *Mol Cell Biol* 2009;29:3229–40. <http://dx.doi.org/10.1128/MCB.01918-08>.
- [52] Weids AJ, Grant CM. The yeast peroxiredoxin Tsa1 protects against protein-aggregate-induced oxidative stress. *J Cell Sci* 2014;127:1327–35. <http://dx.doi.org/10.1242/jcs.144022>.
- [53] Dias L, Pereira-da-Silva S, Tavares M, Malfeito-Ferreira M, Loureiro V. Factors affecting the production of 4-ethylphenol by the yeast *Dekkera bruxellensis* in enological conditions. *Food Microbiol* 2003;20:377–84. [http://dx.doi.org/10.1016/S0740-0020\(03\)00023-6](http://dx.doi.org/10.1016/S0740-0020(03)00023-6).